Microbiology (2011), **157**, 260–269 DOI 10.1099/mic.0.040758-0

Biosynthesis of UDP-xylose and UDP-arabinose in *Sinorhizobium meliloti* 1021: first characterization of a bacterial UDP-xylose synthase, and UDP-xylose 4-epimerase

Xiaogang Gu,[1] Sung G. Lee[1] and Maor Bar-Peled[1,2]

[1]Complex Carbohydrate Research Center (CCRC), University of Georgia, Athens, GA 30602, USA

[2]Department of Plant Biology, University of Georgia, Athens, GA 30602, USA

Correspondence
Maor Bar-Peled
peled@ccrc.uga.edu

Sinorhizobium meliloti is a soil bacterium that fixes nitrogen after being established inside nodules that can form on the roots of several legumes, including *Medicago truncatula*. A mutation in an *S. meliloti* gene (*lpsB*) required for lipopolysaccharide synthesis has been reported to result in defective nodulation and an increase in the synthesis of a xylose-containing glycan. Glycans containing xylose as well as arabinose are also formed by other rhizobial species, but little is known about their structures and the biosynthetic pathways leading to their formation. To gain insight into the biosynthesis of these glycans and their biological roles, we report the identification of an operon in *S. meliloti* 1021 that contains two genes encoding activities not previously described in bacteria. One gene encodes a UDP-xylose synthase (Uxs) that converts UDP-glucuronic acid to UDP-xylose, and the second encodes a UDP-xylose 4-epimerase (Uxe) that interconverts UDP-xylose and UDP-arabinose. Similar genes were also identified in other rhizobial species, including *Rhizobium leguminosarum*, suggesting that they have important roles in the life cycle of this agronomically important class of bacteria. Functional studies established that recombinant SmUxs1 is likely to be active as a dimer and is inhibited by NADH and UDP-arabinose. SmUxe is inhibited by UDP-galactose, even though this nucleotide sugar is not a substrate for the 4-epimerase. Unambiguous evidence for the conversions of UDP-glucuronic acid to UDP-α-D-xylose and then to UDP-β-L-arabinose (UDP-arabinopyranose) was obtained using real-time ^{1}H-NMR spectroscopy. Our results provide new information about the ability of rhizobia to form UDP-xylose and UDP-arabinose, which are then used for the synthesis of xylose- and arabinose-containing glycans.

Received 21 April 2010
Revised 21 July 2010
Accepted 13 September 2010

INTRODUCTION

The plant symbiont *Sinorhizobium meliloti* 1021 is a Gram-negative soil bacterium that induces the formation of nitrogen-fixing nodules on the roots of leguminous plants, including alfalfa, yellow sweet clover and fenugreek (Galibert *et al.*, 2001; van Rhijn & Vanderleyden, 1995). Nodule formation is a multi-step process that is initiated when the bacteria attach to a root hair and cause it to curl. A tubular infection thread is then formed by invagination of the host root cell membrane and allows the bacteria to pass through the root cortex and reach newly formed meristematic cells. These cells then develop into the nodule that contains the nitrogen-fixing bacteroids, which convert atmospheric nitrogen to ammonia and allow the plants to grow in the absence of added nitrogen (Gage, 2004; Jones *et al.*, 2007). There is increasing evidence that changes in the structures and types of the rhizobial cell surface polysaccharides during infection and penetration are required for successful nodulation.

The rhizobial cell surface contains several structurally complex carbohydrates, including extracellular polysaccharides (EPSs), lipopolysaccharides (LPSs), K antigens (capsular polysaccharides; CPSs) and cyclic β-glucans (Carlson *et al.*, 1999). Mutations that impair the production and structure of LPS, CPS and EPS typically affect infection and nodulation (Hirsch, 1999). For example, Campbell *et al.* (2002) have reported that a loss of function mutation in the *S. meliloti lpsB* gene impairs host plant nodulation and leads to the synthesis of an altered LPS containing 40-fold more xylose (Xyl) residues than the

Abbreviations: CPS, capsular polysaccharide; CSL, cellulose synthase-like protein; EPS, extracellular polysaccharide.

The GenBank/EMBL/DDBJ accession numbers for the SmUxs1, SmUxs2 and SmUxe sequences of *Sinorhizobium meliloti* 1021 are GU062741, GU062742 and HM004122, respectively.

Three supplementary tables and four supplementary figures are available with the online version of this paper.

wild-type. However, the biochemical basis for the increased amounts of Xyl residues and the biological function of the altered LPS are unknown.

Several studies have shown that rhizobia synthesize glycans that contain Xyl and arabinose (Ara). For example, polymers containing these pentoses as well as rhamnose (Rha), galactose (Gal) and glucose (Glc) were identified in four rhizobia species (De Leizaola & Dedonder, 1955; Humphrey & Vincent, 1959). Wild-type and mutant strains of *Bradyrhizobium japonicum* grown on gluconate or mannitol produce an EPS comprised of Glc, Gal, Xyl and glucuronic acid (GlcA) (Karr *et al.*, 2000). The LPS isolated from *R. leguminosarum* RBL5523 contains Xyl, 3-deoxy-D-*manno*-2-octulosonic acid (Kdo), galacturonic acid (GalA), mannose (Man), Glc, *N*-acetyl quinovoamine (QuiNAc) and *N*-acetylglucosamine (GlcNAc). The LPS of wild-type *B. japonicum* (Puvanesarajah *et al.*, 1987) contains fucose (Fuc), Xyl, Ara, Man, Glc, *N*-acetylfucosamine, QuiNAc, GlcNAc and Kdo. However, a non-nodulating *B. japonicum* mutant, *HS123*, forms LPS that lacks Xyl and Ara. In addition, partially purified LPS isolated from *R. leguminosarum* 3841 has been reported to contain a glycan named xylomannan, which consists of Man, Xyl and Glc (Forsberg & Carlson, 2008). Moreover, the ratio between Xyl and Man is affected by growth conditions (Kannenberg & Brewin, 1989; Kannenberg *et al.*, 1994; Kannenberg & Carlson, 2001). Taken together, these observations suggest that rhizobia change their cell surface glycans to adapt to changes in their environment. Such changes may be critical for the survival of a rhizobium as a 'free-living' soil bacterium or during its interactions with the host plant root. However, little is known about the biochemical pathways and the corresponding genes involved in these processes. Biosynthesis of glycans requires glycosyltransferases, a class of enzymes that transfer sugar from an activated donor, usually a nucleotide sugar, to an appropriate glycan acceptor, leading to extension of the glycan. To identify genes involved in the synthesis of Ara- and Xyl-containing glycans we decided to investigate nucleotide–sugar biosynthetic genes in rhizobia species.

UDP-Xyl is the sugar donor for the synthesis of diverse Xyl-containing glycans in animals (Götting *et al.*, 2000; Kuhn *et al.*, 2001), fungi (Klutts & Doering, 2008) and plants (Egelund *et al.*, 2006; Peña *et al.*, 2007). UDP-Xyl is formed from UDP-GlcA by a decarboxylation reaction catalysed by UDP-xylose synthase (Uxs) (Bar-Peled *et al.*, 2001; Harper & Bar-Peled, 2002; Hwang & Horvitz, 2002; Pattathil *et al.*, 2005; Zhang *et al.*, 2005). To date, UDP-Ara, which is formed from UDP-Xyl in a reversible reaction catalysed by UDP-xylose 4-epimerase (Uxe) (Burget & Reiter, 1999), has only been identified in green plants, where it is a donor for the synthesis of pectic and hemicellulosic polysaccharides, proteoglycans and glycoproteins (Porchia *et al.*, 2002; Konishi *et al.*, 2007). In contrast, little is known about the formation of activated Xyl and Ara in bacteria and their subsequent use in the synthesis of Xyl- or Ara-containing glycans.

Here we describe the functional characterization of two *S. meliloti* 1021 genes that encode Uxs and Uxe (Fig. 1a). Such enzyme activities have not, to our knowledge, previously been described in bacteria, and thus our data provide the basis for understanding the formation of Xyl- and Ara-containing glycans by rhizobia and their roles in the nodulation of legumes.

METHODS

Cloning of *SmUxs1* and *SmUxe* from *S. meliloti* 1021. Total DNA was isolated from a two-day-old culture of *S. meliloti* 1021 grown in LB liquid medium (2 ml) using phenol/chloroform (Syn & Swarup, 2000). The coding sequences of SMb20458 (herein named UDP-xylose synthase, *SmUxs1*) and SMb20459 (herein named UDP-xylose 4-epimerase, *SmUxe*) were PCR-amplified using 1 unit of proof-reading Platinum *Taq* DNA polymerase high-fidelity (Invitrogen), 0.2 μM of each forward and reverse primer (for Uxs1, 5′-TCATGAATTATTTT-AGAAATGACTTCAG-3′ and 5′-AAGCTTGACCAGCTCCGCCTT-TCC-3′; for Uxe, 5′-CCATGGTTGCGCCACGTATCCTCGTC-3′ and 5′-GGATCCAAGCTTTGACCGGACCTCCAGC-3′), 200 μM dNTPs and *S. meliloti* 1021 DNA as template. Each PCR product was separated by agarose gel electrophoresis, extracted and then cloned to generate plasmids pGEM-T : SmUxs1#2 and pCR4 : SmEPI#2, respectively. Following DNA sequence analyses and subsequent biochemical characterization (see below) of the cloned genes, they were annotated as SmUxs1 and SmUxe, and their sequences were deposited in GenBank. The *Bsp*HI–*Hin*dIII fragment (1053 bp) containing the full-length *SmUxs1* gene and the *Nco*I–*Hin*dIII fragment (986 bp) containing the full-length *SmUxe*, both without stop codons, were cloned into an *Escherichia coli* expression vector (pET28b : SmUxs1#1 and pET28b : SmUxe#1) for the production of recombinant proteins with a six-histidine extension at the C terminus.

Expression and purification of recombinant SmUxs1 and SmUxe. *E. coli* cells containing pET28b : SmUxe#1 or an empty vector (pET28b) were cultured for 16 h at 37 °C in LB medium (10 ml) supplemented with kanamycin (50 μg ml^{-1}) and chloramphenicol (34 μg ml^{-1}). A portion (8 ml) of the cultured cells was transferred into fresh LB liquid medium (250 ml) supplemented with the same antibiotics, and the cells were then grown at 37 °C at 250 r.p.m. until the cell density reached OD_{600} 0.8. Gene expression was then induced by the addition of IPTG (to 0.5 mM), and the cells were then grown for 4 h at 30 °C at 250 r.p.m. Overnight cultures of cells harbouring pET28b : SmUxs1#1 or an empty vector (pET28) were transferred into 190 ml fresh *E. coli* Expression Medium (Invitrogen) supplemented with kanamycin (50 μg ml^{-1}) and chloramphenicol (34 μg ml^{-1}), and grown for 24 h at 30 °C at 250 r.p.m. The induced cells were collected by centrifugation (6000 ***g*** for 10 min at 4 °C), suspended in 20 ml lysis buffer [50 mM sodium phosphate, pH 7.5, containing 10 % (v/v) glycerol, 1 mM EDTA, 1 mM DTT and 0.5 mM PMSF] and lysed in an ice bath by sonication (24 cycles of 10 s on, 20 s off) using a Misonix S-4000 sonicator (Misonix) equipped with a microtip probe. The lysed cells were centrifuged at 6000 ***g*** for 10 min at 4 °C. The supernatant was supplemented with 1 mM DTT and centrifuged again (30 min at 20 000 ***g***). The resulting supernatant (termed S20) was recovered and kept at −20 °C. His-tagged proteins were purified using a Ni-Sepharose fast-flow column [2 ml resin (GE Healthcare Life Sciences) that had been packed in a 10 mm internal diameter × 150 mm column]. The column was pre-equilibrated with loading buffer [50 mM sodium phosphate (pH 7.5), 0.3 M NaCl]. The bound His-tagged protein was eluted with the same buffer containing an increasing amount of imidazole (10–250 mM). Fractions containing

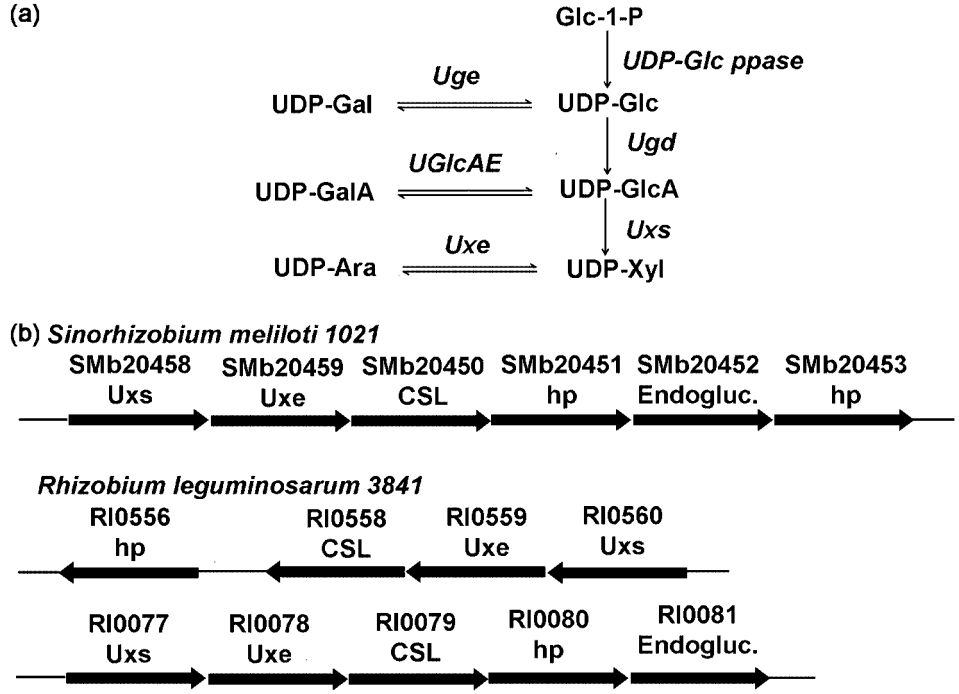

Fig. 1. Biosynthesis of UDP-Xyl and UDP-Ara in rhizobia. (a) In rhizobia, UDP-glucose pyrophosphorylase (UDP-Glc ppase) converts glucose 1-phosphate (Glc-1-P) and UTP to UDP-Glc. UDP-Glc and UDP-Gal are interconverted by UDP-glucose 4-epimerase (Uge) [exoB (Sánchez-Andújar *et al.*, 1997)]. UDP-glucose 6-dehydrogenase (Ugd) [exo5 (Laus *et al.*, 2004)] converts UDP-Glc and NAD^+ to UDP-GlcA and NADH. UDP-GlcA and UDP-GalA are interconverted by UDP-glucuronic acid 4-epimerase (UGlcAE) [lpsL (Keating *et al.*, 2002)]. UDP-GlcA is decarboxylated to give UDP-Xyl by UDP-xylose synthase (Uxs; this study). UDP-Xyl and UDP-Ara are interconverted by UDP-xylose 4-epimerase (Uxe; this study). (b) Organization of some of the operons containing Uxs and Uxe genes in *S. meliloti* 1021 and *R. leguminosarum* 3841. The locus number for each gene within the operon is shown and the annotated function is indicated below. The biochemical functions of SMb20458 and SMb20459 based on this report are UDP-xylose synthase (SmUxs1) and UDP-xylose 4-epimerase (SmUxe), respectively. The *R. leguminosarum* 3841 genes RI0560 and RI0077 encode active Uxs, and RI0559 and RI0078 encode active Uxe (S. Roy, X. Gu & M. Bar-Peled, unpublished data). hp, hypothetical protein; Endogluc., endoglucanase.

the desired enzymic activity were pooled, supplemented with 10 % (v/v) glycerol and 5 mM DTT, and then dialysed (6000–8000 molecular mass cut-off, Spectrum Laboratories) three times for 30 min at 4 °C against 50 mM sodium phosphate, pH 7.5, containing 0.1 M NaCl, 10 % (v/v) glycerol and 5 mM DTT. The dialysate was flash-frozen in liquid nitrogen and stored at −80 °C. Proteins extracted from *E. coli* cells expressing the empty vector were obtained using the same column purification protocol and were used as controls in enzyme assays and SDS-PAGE analyses. Protein concentrations were determined using the Bradford reagent with BSA as standard. The native molecular mass of each recombinant protein was estimated by size-exclusion chromatography, as described previously (Gu *et al.*, 2010).

Uxs, Uxe enzyme assays, HPLC and NMR product analyses. Standard Uxs reactions (50 µl final volume) contained 50 mM sodium phosphate (pH 7.6), 1 mM NAD^+, 1 mM UDP-GlcA and 0.3 µg purified recombinant SmUxs1. Uxe reactions (50 µl final volume) contained 50 mM sodium phosphate (pH 7.6), 0.5 mM NAD^+, 0.5 mM UDP-Xyl and 0.04 µg purified recombinant SmUxe. Reactions were kept for up to 30 min (Uxs) or 10 min (Uxe) at 37 °C and then terminated by heating for 45 s at 100 °C. Chloroform (50 µl) was then added and the mixture was vortexed for 30 s. The suspension was centrifuged at room temperature for 5 min at 14 000 ***g*** and the upper aqueous phase was collected. Reaction products for SmUxs1 were chromatographed on a Q15 anion-exchange column (2 mm × 250 mm, Amersham) using an Agilent 1100 Series HPLC system equipped with an autosampler, diode-array detector and ChemStation software. Reaction products for SmUxe were chromatographed on a Prep C18 Scalar column (4.6 mm internal diameter × 250 mm, Agilent) at a flow rate of 1 ml min^{-1} using a gradient from solution A (20 mM *tert*-butylamine-H_3PO_4, pH 6.6, 2 %, v/v, acetonitrile) to solution B (20 mM *tert*-butylamine-H_3PO_4, 20 %, v/v, acetonitrile) over 35 min. Nucleotides were detected by their UV absorbance, and the maximum absorbances for UDP-sugars and NAD^+ were at 261 and 259 nm, respectively. The amount of product formed was determined using calibration curves of standard UDP-Xyl and UDP-GlcA. The products formed by the Uxs reaction (eluted at 16.8 min from Q-column) and the Uxe reaction (eluted at 8.2 min from the C18 column) were collected, lyophilized, dissolved in 99.9 % D_2O and analysed by ^{1}H-NMR spectroscopy. UDP-Xyl and UDP-Ara were purchased from CarboSource Services (CCRC); UDP-GlcA, UDP-Glc and NAD^+ were obtained from Sigma.

Real-time ^{1}H-NMR enzymic reaction assays (200 µl) were performed at 37 °C in a final mixture of D_2O : H_2O (1 : 9, v/v), and contained 50 mM sodium phosphate, pH/pD 7.6, 1 mM UDP-GlcA, 1 mM NAD^+ and 1.2 µg recombinant SmUxs1. The NMR assay for SmUxe (0.16 µg) used the same buffer, with NAD^+ and 1 mM UDP-Xyl.

Real-time ^{1}H-NMR spectra were obtained using a Varian DirectDrive spectrometer operating at 900 or 600 MHz. Data acquisition was started between 5 and 10 min after the addition of enzyme to allow spectrometer acquisition conditions to be optimized. Sequential 1D proton spectra with pre-saturation of the water resonance were acquired over the course of the enzymic reaction. All chemical shifts (p.p.m.) are referenced to 2,2-dimethyl-2-silapentane-5-sulphonate.

Characterization and kinetic analyses of the recombinant enzymes. SmUxs1 and SmUxe activities were determined using different buffers, different temperatures, and in the presence of selected cations or potential inhibitors. For optimal pH studies, solutions of recombinant SmUxs1 (0.3 μg) were mixed in each individual buffer (50 mM). Subsequently, NAD^+ (1 mM) and UDP-GlcA (1 mM) were added and reactions were incubated for 30 min at 37 °C. Inhibition assays were performed by first mixing the enzyme and buffer with various additives (e.g. nucleotides) on ice for 10 min. UDP-GlcA and NAD^+ (1 mM each) were then added. After 30 min at 37 °C, the amount of UDP-Xyl formed was determined by Q15 anion-exchange chromatography. Optimal temperature studies were performed using standard conditions for 30 min at different temperatures, and the amount of UDP-Xyl was determined by HPLC. SmUxe (0.04 μg protein) was characterized in a similar manner using 10 min reactions with NAD^+ (0.5 mM) and UDP-Xyl (0.5 mM), and the products were analysed by reverse-phase HPLC.

The catalytic activity of SmUxs1 (0.3 μg) or SmUxe (0.04 μg) was determined at 37 °C for 8 min (Uxs) or 5 min (Uxe) in 50 mM sodium phosphate, pH 7.6, containing 1 mM NAD^+, with variable concentrations (0.08–1 mM) of UDP-GlcA (Uxs) or UDP-Xyl (Uxe). K_m values were calculated from a plot of the reciprocal initial velocity against the reciprocal UDP-sugar concentration.

RESULTS

Identification and cloning of *S. meliloti* 1021 UDP-xylose synthase 1 (SmUxs1) and UDP-xylose 4-epimerase (SmUxe)

BLAST searches using the amino acid sequence of *Arabidopsis* UDP-xylose synthase (AtUxs3, GenBank accession number AF387789) identified two *S. meliloti* 1021 Uxs homologues (*SmUxs1* and *SmUxs2*; see Supplementary Fig. S1). Both homologues reside on the 1.68 Mb pSymb megaplasmid of *S. meliloti* 1021. SmUxs1 has 59, 55 and 57 % amino acid sequence identity to known plant, fungal and human Uxs, respectively. The operon containing *SmUxs1* (SMb20458) has an additional gene (SMb20459, herein named *SmUxe*). This gene encodes a protein with 41, 42 and 44 % amino acid sequence identity to human, yeast and *Burkholderia* UDP-galactose 4-epimerases, respectively, and 42 % amino acid sequence identity to the *Arabidopsis* UDP-xylose 4-epimerase (MUR4, At1g30620; Burget *et al.*, 2003) (Supplementary Fig. S2). Such sequence identity, however, is insufficient to predict the function of SMb20459. Nonetheless, a comparison of the *SmUxs1* operon with other sequenced rhizobial genomes identified similar genes and operons (see Fig. 1b), suggesting the widespread occurrence of these genes.

To determine whether the *S. meliloti* homologues (SmUxs1 and SmUxe) function as a UDP-xylose synthase and as a UDP-sugar epimerase, we cloned and expressed both genes in *E. coli* and then determined the biochemical properties of the recombinant proteins.

SmUxs1 encodes active UDP-xylose synthase; *SmUxe* encodes active UDP-xylose 4-epimerase

A clearly visible protein band (~40 kDa) was detected by SDS-PAGE analysis of the extracts from *E. coli* cells expressing recombinant SmUxs1 (Fig. 2a, lane 1) but was absent in *E. coli* cells expressing the empty vector. The expressed protein was purified (Fig. 2a, lane 3) and shown, using an HPLC-based assay, to convert UDP-GlcA to a new UDP-sugar in the presence of NAD^+. The newly formed UDP-sugar had the same retention time (16.8 min) as the UDP-Xyl standard (Fig. 2b, panel 3, indicated by an asterisk), and its ^{1}H-NMR spectrum (Fig. 3a, Supplementary Table S1) was consistent with UDP-Xyl. The distinct chemical shift (Supplementary Table S1) of H″1 at 5.51 p.p.m. and the coupling constant value of 7.0 Hz for $J_{1',P}$ show the linkage of the anomeric Xyl residue with the phosphate of UDP. The coupling constant value of 3.4 Hz for $J_{1',2'}$ and the $J_{2',3'}$, $J_{3',4'}$ values of 9.5 and 9.5 Hz, respectively, indicate an α-xylopyranose configuration. The collective analyses thus confirm that the recombinant SmUxs1 is a UDP-xylose synthase, as illustrated in Fig. 1(a).

We next analysed the enzymic function of recombinant SmUxe. The protein was expressed and purified from *E. coli* (Fig. 4a, lanes 1 and 3). Initial HPLC-based assays determined that SmUxe was unable to epimerize UDP-Glc or UDP-Gal, even when the reactions were performed for extended times (data not shown). However, SmUxe readily converted UDP-Xyl to a new UDP-sugar that had the same retention time (8.2 min) as UDP-Ara (see Fig. 4b, panels 2 and 3). Proteins isolated from *E. coli* cells expressing empty vector had no activity (Fig. 4b, panels 5 and 6). The ^{1}H-NMR spectrum of the product eluting at 8.2 min (Fig. 3b, Supplementary Table S1) contained a signal for an anomeric proton at 5.59 p.p.m. ($J_{1',2'}$ 3.4 Hz; $J_{1',P}$ 6.8 Hz), and had $J_{2',3'}$ (10 Hz), $J_{3',4'}$ (3.4 Hz), $J_{4,5a'}$ (1.8 Hz), $J_{4,5b'}$ (<1 Hz), and $J_{5a',5b'}$ (12.9 Hz) values (Fig. 4b, panel 3) that were consistent with UDP-β-L-arabinopyranose (UDP-Ara). SmUxe also converted UDP-Ara to a peak that eluted at 8.9 min (Fig. 4c, panels 2 and 3). The ^{1}H-NMR spectrum of this product (Fig. 4c, panel 3) was identical to that of UDP-Xyl. Together, these data establish that recombinant SmUxe is a 4-epimerase that interconverts UDP-D-xylopyranose and UDP-β-L-arabinopyranose (Fig. 1a, Supplementary Table S1). Thus, we conclude that *S. meliloti* has genes that encode proteins forming UDP-Xyl and UDP-Ara from UDP-GlcA.

Real-time NMR assays of SmUxs1 and SmUxe activity

Time-resolved NMR-based assays were performed with SmUxs1 or SmUxe and their corresponding substrates to monitor product formation and the presence of intermediates. The enzymic progression of SmUxs1, as monitored by

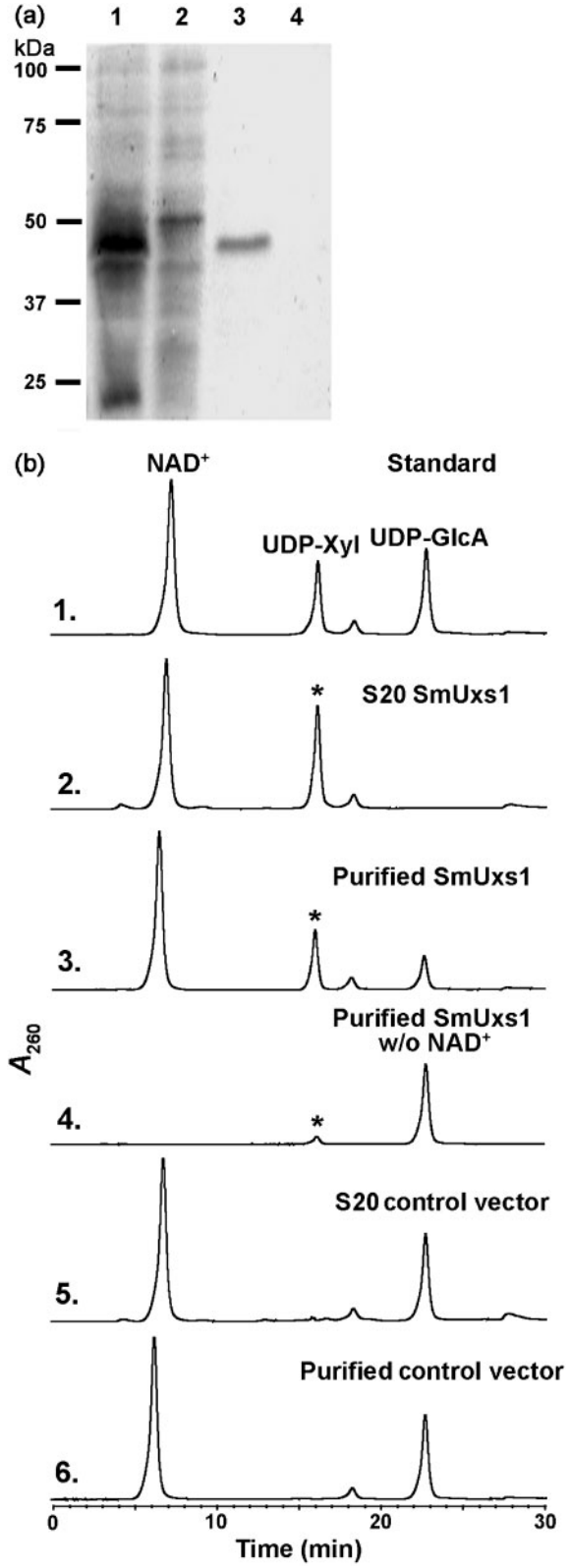

Fig. 2. Expression and characterization of recombinant SmUxs1. (a) SDS-PAGE of total soluble protein isolated from *E. coli* cells expressing SmUxs1 (lane 1), control empty vector (lane 2), and column-purified SmUxs1 or control (lanes 3 and 4, respectively). (b) High-performance anion-exchange chromatography of the products formed by SmUxs1. Purified recombinant SmUxs1 was reacted with UDP-GlcA for 45 min in the presence (panel 3) or absence (panel 4) of added NAD^+. The corresponding column-purified protein isolated from cells expressing the empty vector was reacted with UDP-GlcA and NAD^+ for 45 min (panel 6) as a control. The reaction products were separated on a Q15 anion-exchange column. The distinct UDP-sugar peak indicated by an asterisk (panels 2 and 3 with the same retention time as UDP-Xyl) was collected and characterized by ^{1}H-NMR spectroscopy. The activity of total soluble protein (S20) isolated from cells expressing recombinant SmUxs1 (panel 2) or vector control (panel 5) is shown.

analysing selected regions of the NMR spectra, is shown in Fig. 5. The characteristic NMR signal having a quadruplet peak that corresponds to the C1-anomeric proton of UDP-GlcA (G) (labelled G1′ at 5.58 p.p.m. in Fig. 5b; and in an expansion of this region in Fig. 5c) was decreased, and simultaneously the quadruplet peak signal corresponding to the UDP-Xyl anomeric proton (X1′, 5.51 p.p.m.) was increased during the time-course of the Uxs reaction. No variation was observed for the peaks corresponding to NAD^+ (N) protons, as expected. In addition, performing the assay at a higher field strength (900 MHz) led to a better resolution of signals and product identification, showing clear differences in the chemical shifts for the proton attached to the C-6 of uracil during the formation of UDP-Xyl from UDP-GlcA (Fig. 5d, marked by X6 and G6, respectively).

The real-time ^{1}H-NMR spectra the of SmUxe assay (see Supplementary Fig. S3) revealed that the Xyl H-1 signal of UDP-Xyl (X1′) decreased with a concomitant increase in the Ara H-1 signal of UDP-Ara (A1′). The appearance of signals with chemical shifts corresponding to H-5 ($A5_a'$, 3.71 p.p.m.) and H-4 (A4′, 4.01 p.p.m.) of the arabinosyl moiety provides additional evidence for the formation of UDP-Ara. In addition, NMR established that NAD^+ is not released from the epimerase during the C-4 oxidation ($NAD^+ \rightarrow NADH$)/reduction ($NADH \rightarrow NAD^+$) cycle.

We then used real-time ^{1}H-NMR to monitor the product formation when SmUxs1 and SmUxe were reacted together with UDP-GlcA. The conversion of UDP-GlcA to UDP-Xyl was immediately apparent (Supplementary Fig. S4; 5.6–5.5 p.p.m.). As the reaction progressed, the UDP-Xyl was inter-converted to UDP-Ara, until UDP-GlcA was completely consumed and an equilibrium between UDP-Xyl and UDP-Ara was achieved. At equilibrium, the ratio of UDP-Ara to UDP-Xyl was 0.8 (Table 1). Overall, the real-time NMR-based enzyme assay provides a powerful analytical tool to observe the transformation of nucleotide sugars.

Characterization and properties of recombinant SmUxs1 and SmUxe

The recombinant *SmUxs1* gene encodes a polypeptide with a molecular mass of ~40 kDa. However, the functional

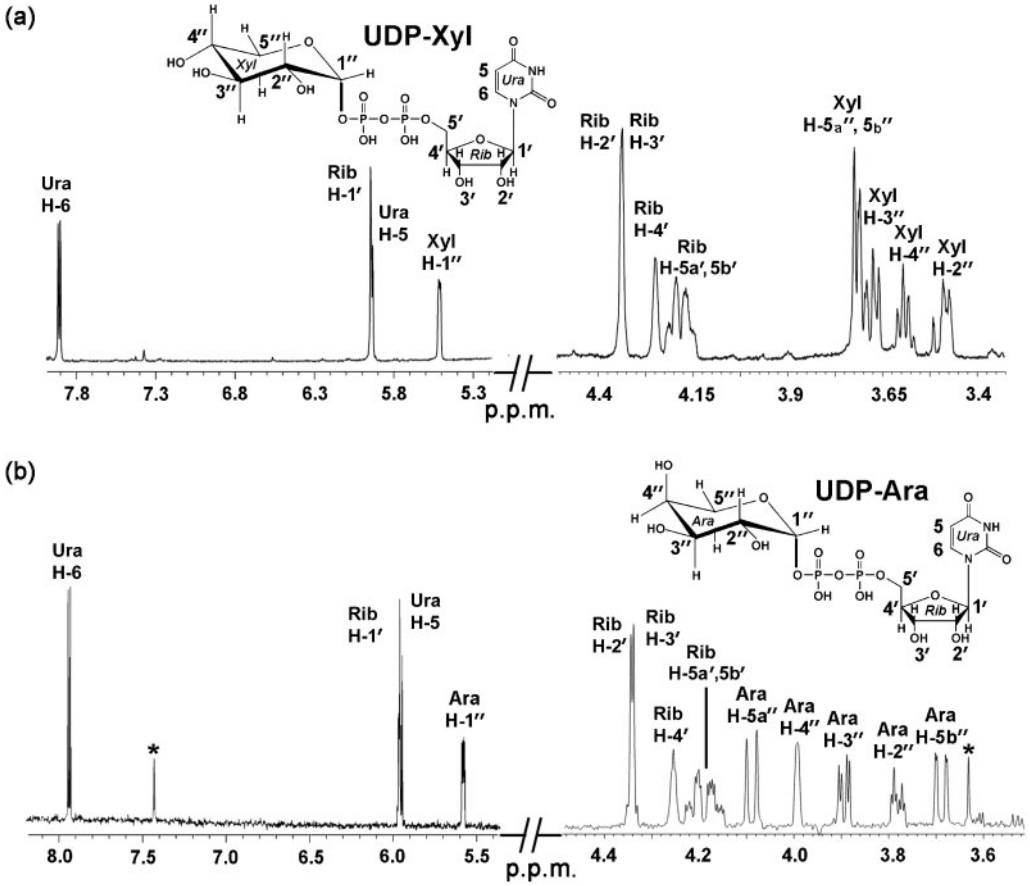

Fig. 3. ^{1}H-NMR spectroscopic analyses of the UDP-α-D-xylose and UDP-β-L-arabinose formed by SmUxs1 and SmUxe, respectively. (a) The peak (Fig. 2b, panel 2, marked by an asterisk) corresponding to the product formed by SmUxs1 was collected and analysed by ^{1}H-NMR spectroscopy at 600 MHz. Portions of the NMR spectrum between 3.4–4.5 and 5.2–8.0 p.p.m. are shown. The assigned signals have the symbol H for the uracil protons (Ura), the symbol H′ for the ribose (Rib) protons, and the symbol H″ for the xylose (Xyl) protons. (b) The Uxe enzymic product (Fig. 4b, panel 2, marked with an asterisk) was collected from the column, lyophilized and analysed by ^{1}H-NMR at 25 °C. The 600 MHz NMR spectrum of the product is shown between 3.5–4.5 and 5.4–8.2 p.p.m. The assigned signals have the symbol H for the uracil protons (Ura), the symbol H′ for the ribose (Rib) protons, and the symbol H″ for the arabinose (Ara) protons.

SmUxs1 protein elutes from a size-exclusion column in the region for a ~75 kDa protein (Table 1), suggesting that it exists as a dimer. The SmUxe polypeptide (~37 kDa) also eluted from the column as a dimer (Table 1). Kinetic data for SmUxs1 and SmUxe are summarized in Table 1. SmUxs1 had an apparent K_m of 94.8 μM (UDP-GlcA) and a k_{cat}/K_m value (s^{-1} mM^{-1}) of 18.3. SmUxe had an apparent K_m value of 0.31 mM for UDP-Xyl and a k_{cat}/K_m value (s^{-1} mM^{-1}) of 42.1 (Table 1).

Recombinant SmUxs1 and SmUxe had optimal pH values of 8.0 and 7.6, respectively, in phosphate buffer, and their optimal temperature was 37 °C (Table 1). Both enzymes were fully active in the presence of EDTA (data not shown), suggesting that metal ions are not required for SmUxs1 and SmUxe activity. Similar to the Uxs1p from the fungus *Cryptococcus neoformans* (Bar-Peled *et al.*, 2001) but distinct from the plant Uxs homologues (Harper & Bar-Peled, 2002; Pattathil *et al.*, 2005), the activity of *S. meliloti* Uxs1 was inhibited by NADH (Supplementary Table S2). UDP-Ara also inhibited SmUxs1 although it does not inhibit known plant and fungal Uxs. Thus, in *S. meliloti* 1021, UDP-Ara may control the GlcA→Xyl→Ara pathway by feedback inhibition. Both SmUxe and SmUxs1 require the co-factor NAD^+. However, SmUxe, in contrast to SmUxs, is not inhibited by NADH (Supplementary Table S3). This suggests that SmUxe has a stronger interaction with the co-factor than SmUxs1. Moreover, SmUxs1 does not utilize $NADP^+$ as a co-factor, suggesting that the enzyme requires the ribosyl C2-OH for activity.

No decarboxylation activity was observed when SmUxs1 reacted for up to 60 min with UDP-GalA, which is an isomer of UDP-GlcA, suggesting that the recombinant enzyme is substrate specific. In addition, SmUxe had no detectable activity when reacted with different nucleotide

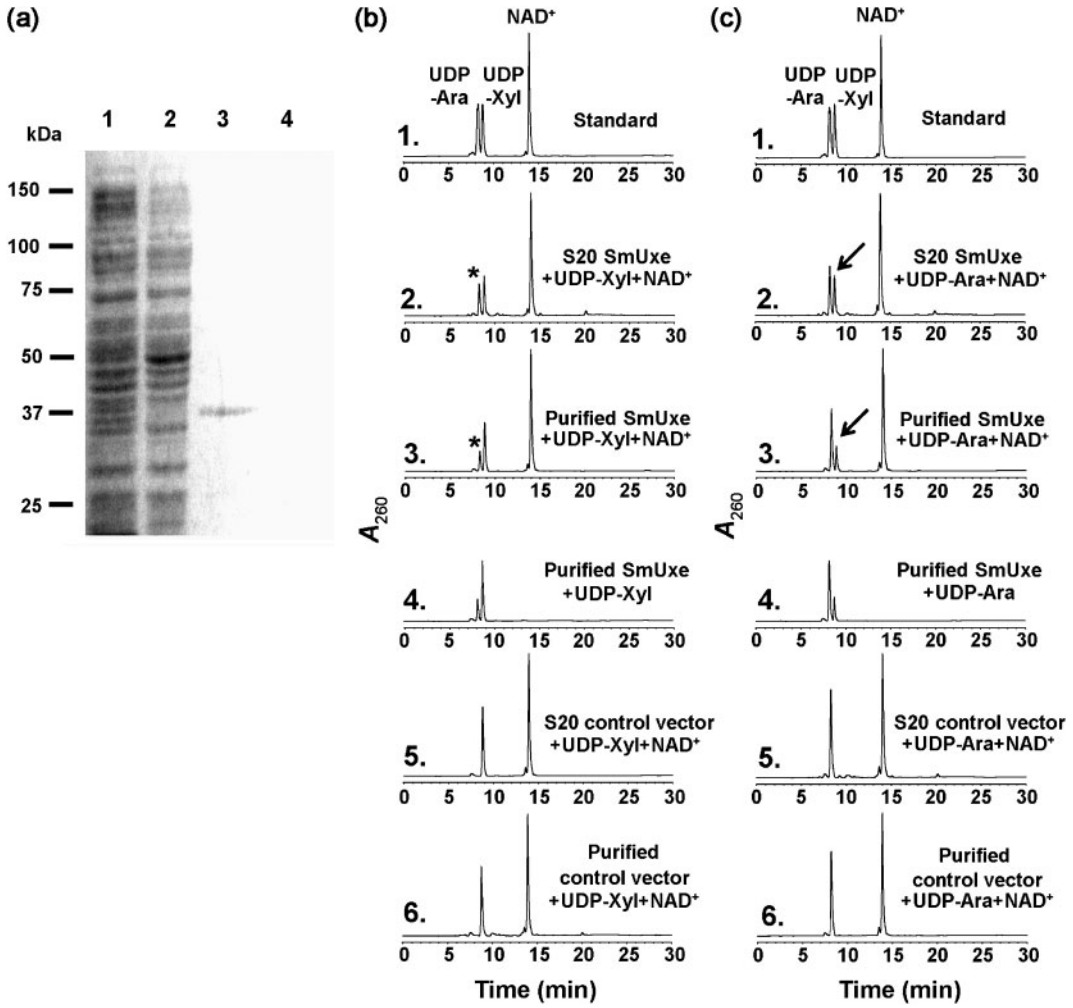

Fig. 4. Expression and characterization of recombinant SmUxe. (a) SDS-PAGE of total soluble protein isolated from *E. coli* cells expressing SmUxe (lane 1), control empty vector (lane 2), and column-purified SmUxe or control (lanes 3 and 4, respectively). (b) High-performance reverse-phase chromatography of the products formed by SmUxe reacting with UDP-Xyl. Purified recombinant SmUxe was reacted with UDP-Xyl for 45 min in the presence (panel 3) or absence (panel 4) of added NAD^+. The purified protein isolated from cells expressing control empty vector was incubated with UDP-Xyl and NAD^+ for 45 min (panel 6) and is a control. The distinct UDP-sugar peak marked by the asterisk (panels 2 and 3 with the same retention time as UDP-Ara) was collected and analysed by ^{1}H-NMR spectroscopy. The activity of total soluble protein (S20) isolated from cells expressing recombinant SmUxe (panel 2) or vector control (panel 5) is shown. (c) High-performance reverse-phase chromatography of the products formed by SmUxe reacting with UDP-Ara. Purified recombinant SmUxe was reacted with UDP-Ara for 45 min in the presence (panel 3) or absence (panel 4) of exogenous NAD^+. The purified protein isolated from cells expressing control empty vector was incubated with UDP-Xyl and NAD^+ for 45 min (panel 6) and is a control. The peak marked by the arrows (panels 2 and 3 with the same retention time as UDP-Ara) was collected and analysed by ^{1}H-NMR spectroscopy. The activity of total soluble protein (S20) isolated from cells expressing recombinant SmUxe (panel 2) or vector control (panel 5) is shown.

sugars, including UDP-Glc, UDP-GlcA, UDP-GalA, UDP-GlcNAc and GDP-Man (data not shown).

DISCUSSION

Our study describes the functional characterization of recombinant *S. meliloti* 1021 Uxs1 and Uxe, and thus provides biochemical evidence for genes that are involved in producing UDP-Ara and UDP-Xyl in bacteria.

Two Uxs genes located in different operons were identified in *S. meliloti* 1021. BLAST analyses revealed that the *R. leguminosarum* 3841 genome contains three Uxs homologues (RL0560, RL0077 and PRL90147) located in different operons. Preliminary studies suggest that RL0560 and RL0077 encode active Uxs (S. Roy, X. Gu & M. Bar-Peled, unpublished data). One possibility for the existence of two Uxs isoforms in *S. meliloti* 1021 is that each SmUxs functions at different stages of the *Sinorhizobium* life cycle.

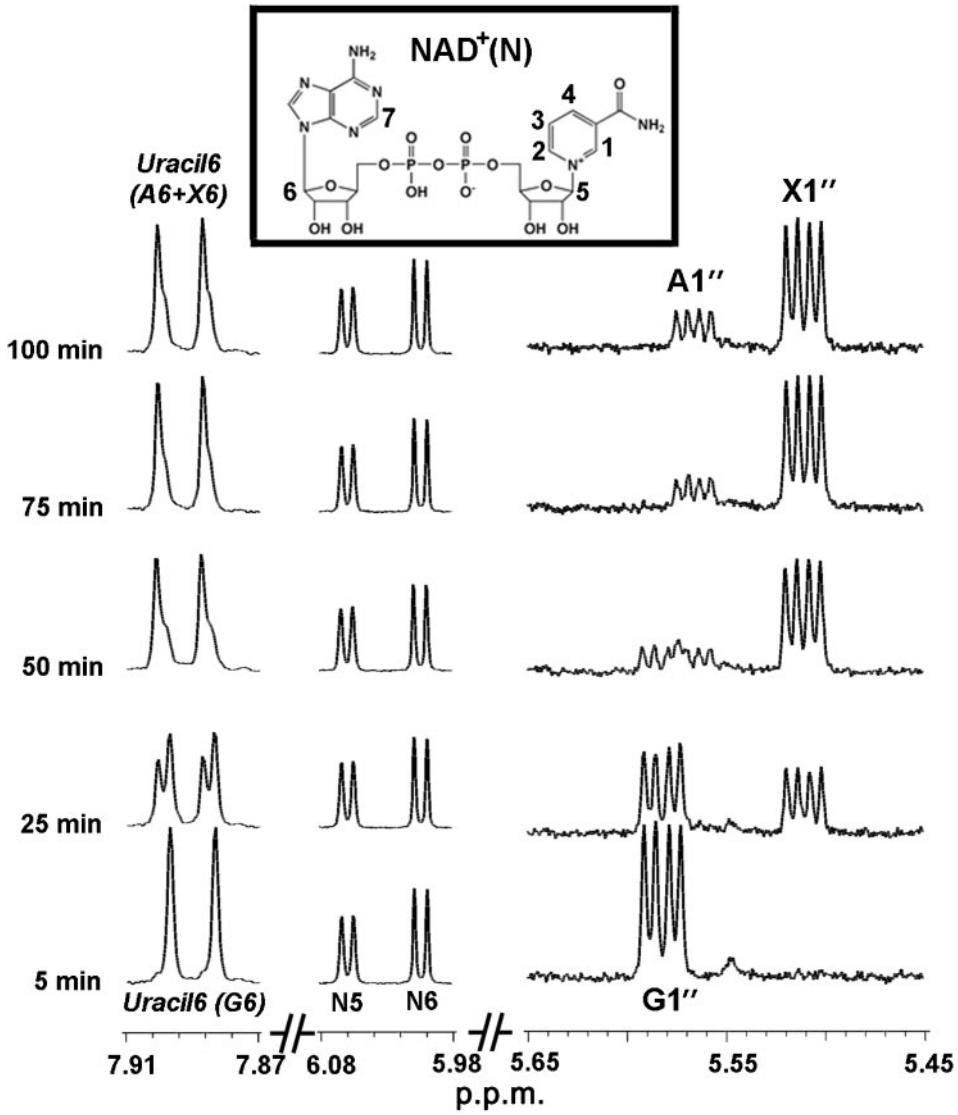

Fig. 5. Real-time ^{1}H-NMR analyses of dual-enzyme (SmUxe and SmUxs1) activities. SmUxe and SmUxs1 were mixed with UDP-GlcA and NAD^{+}. Approximately 5 min after enzyme addition and NMR shimming, NMR data were collected at 37 °C using the 600 MHz spectrometer (bottom trace). Selected regions of the spectra acquired between 5 and 100 min are shown. ^{1}H-NMR signals for the H-1 proton of UDP-GlcA, UDP-Xyl and UDP-Ara (from 5.45 to 5.65 p.p.m., quadruplet peak) are labelled as G1″, X1″ and A1″, respectively. The N5, N6 protons of NAD^{+} (5.98–6.08 p.p.m.) are labelled arbitrarily as shown in the insert. Peaks marked by *Uracil6 (A6+X6)* (7.87–7.91 p.p.m.) are the mixture of signals from the H-6 proton of the uracil of UDP-Xyl and UDP-Ara.

No data are currently available to evaluate the transcription level of specific SmUxs at different developmental stages. However, such a possibility could be supported by examining the data from large microarray analyses (Karunakaran *et al.*, 2009) of many rhizobial genes, including the Uxs homologues in *R. leguminosarum* 3841. Transcriptomic data for the three *R. leguminosarum* Uxs genes (RL0560, RL0077 and PRL90147) indicate that the expression of RL0560, but not RL0077 and PRL90147, is upregulated approximately fivefold in a 15-day pea-bacteroid when compared with free-living bacteria (Karunakaran *et al.*, 2009).

Both *S. meliloti* 1021 and *R. leguminosarum* 3841 operons carrying Uxs and Uxe genes also contain a gene encoding a protein with homology to a cellulose synthase-like protein (CSL) (Fig. 1b), suggesting that they provide UDP-Xyl and UDP-Ara for the formation of specific glycans. These glycans, for example, could be the Ara- and Xyl-containing glycans found in the viscous EPSs, the nodule-specific polysaccharide (NPS), the CPS or the altered LPS structure that is displayed under acidic conditions. In addition, it is possible that upregulation of Uxs gene(s) accounts for the 40-fold increase of xylosyl residues and lack of GalA and

Table 1. Enzymic properties of recombinant SmUxs1 and SmUxe

Property	SmUxs1	SmUxe
Optimal pH	7.6–8.4	7.6–8.0
Optimal temperature (°C)*	37	37
K_m (mM)†	0.095 ± 0.003	0.31 ± 0.05
V_{max} (μM s^{-1})	0.25 ± 0.01	0.25 ± 0.04
k_{cat} (s^{-1})	1.7 ± 0.1	13.0 ± 1.9
k_{cat}/K_m (mM^{-1} s^{-1})	18.3 ± 0.2	42.1 ± 1.7
Mass of active protein/monomer (kDa)‡	75/40.5	66/36.7
Equilibrium constant§	–	0.80 ± 0.01

*Optimal temperature assays were conducted in phosphate buffer.
†The reciprocal initial velocity was plotted against the reciprocal UDP-sugar concentration according to Lineweaver and Burk to calculate the corresponding K_m values. The data presented are the mean K_m values from three experiments.
‡The mass of active SmUxs1 or SmUxe eluted from a Superdex-200 gel filtration column (28.7 or 29.3 min, respectively) was estimated based on extrapolation (R^2=0.981) from the relative time for a standard protein marker.
§The ratio between UDP-Ara and UDP-Xyl for SmUxe activity was determined after a 4 h assay.

GlcA residues in the 'modified LPS glycan' prepared from the *S. meliloti* 1021 *lpsB* mutant (Campbell *et al.*, 2002). The increased production of Uxs enzymes in the *lpsB* mutant may alter the UDP-GalA and UDP-GlcA pool by driving the formation of UDP-Xyl (Fig. 1a) and its incorporation into the modified LPS.

SmUxs1 requires NAD^+ for the oxidative decarboxylation of UDP-GlcA. Many short-chain dehydrogenase/reductases (SDR proteins) also require NAD^+ for activity. In some of these enzymes, the co-factor is tightly bound to the enzyme during the catalytic oxidation and reduction steps ($NAD^+ \rightarrow NADH \rightarrow NAD^+$). However, other SDR enzymes do not bind NAD^+ tightly and the co-factor is typically lost during purification. The extent of binding between NAD^+ and Uxs from animals, plants and fungi is typically assessed by the inhibition effects of NADH. For example, Uxs1p from *C. neoformans* and SmUxs1 are both inhibited by NADH, whereas the plant and animal Uxs enzymes characterized to date are not (Harper & Bar-Peled, 2002; Hwang & Horvitz, 2002; Pattathil *et al.*, 2005; Zhang *et al.*, 2005). The 'binding stringency' of the enzyme to NAD^+ has been reported to be determined by the number of hydrogen bonds formed between specific amino acid residues and the co-factor. For example, Thoden *et al.* (1996) have proposed that 17 hydrogen bonds are required for the tight binding between NAD^+ and UDP-glucose 4-epimerase. In contrast, the six hydrogen bonds that have been proposed to mediate the interaction between NAD^+ and ArnA (Gatzeva-Topalova *et al.*, 2005) are not sufficient to retain the co-factor during enzyme purification.

Some bacteria utilize Ara as a carbon source (Ricke *et al.*, 1996), whereas other bacteria, including *Salmonella typhimurium* and *E. coli*, produce UDP-β-4-deoxy-4-formamido-L-arabinose via decarboxylation of UDP-GlcA (Breazeale *et al.*, 2002). As far as we are aware, there have been no previous reports of a bacterial 4-epimerase that interconverts UDP-Xyl and UDP-Ara. Preliminary studies suggest that the Uxe homologues from *R. leguminosarum* 3841 are also specific for these UDP-pentoses (S. Roy, X. Gu & M. Bar-Peled, unpublished data). Thus, it is likely that Uxs and Uxe genes involved in UDP-Xyl and UDP-Ara synthesis exist in rhizobial species that produce Xyl- and Ara-containing glycans.

In summary, the functional identification of bacterial enzymes involved in UDP-Xyl and UDP-Ara biosynthesis, along with the existence of putative glycosyltransferases in the same operons, provides the basis to elucidate the pathway for these glycans in rhizobia. Work is currently under way to determine whether the CSL gene in the operon encodes a functional glycosyltransferase.

ACKNOWLEDGEMENTS

We thank Dr John Glushka for his help with NMR spectroscopy, and Malcolm O'Neil for constructive comments on the manuscript. This research was supported in part by the National Science Foundation (NSF) IOB-0453664 (to M. B.-P.) and by the BioEnergy Science Center (grant DE-PS02-06ER64304), which is supported by the Office of Biological and Environmental Research in the Department of Energy (DOE) Office of Science. This research also benefited from activities at the South-East Collaboratory for High-Field Biomolecular NMR, a research resource at the University of Georgia, funded by the National Institute of General Medical Sciences (NIGMS grant number GM66340) and the Georgia Research Alliance. This research was also supported in part by the DOE-funded Center for Plant and Microbial Complex Carbohydrates (DE-FG05-93ER20097).

REFERENCES

Bar-Peled, M., Griffith, C. L. & Doering, T. L. (2001). Functional cloning and characterization of a UDP-glucuronic acid decarboxylase: the pathogenic fungus *Cryptococcus neoformans* elucidates UDP-xylose synthesis. *Proc Natl Acad Sci U S A* **98**, 12003–12008.

Breazeale, S. D., Ribeiro, A. A. & Raetz, C. R. (2002). Oxidative decarboxylation of UDP-glucuronic acid in extracts of polymyxin-resistant *Escherichia coli*. Origin of lipid A species modified with 4-amino-4-deoxy-L-arabinose. *J Biol Chem* **277**, 2886–2896.

Burget, E. G. & Reiter, W. D. (1999). The *mur4* mutant of *Arabidopsis* is partially defective in the de novo synthesis of uridine diphospho L-arabinose. *Plant Physiol* **121**, 383–389.

Burget, E. G., Verma, R., Molhoj, M. & Reiter, W. D. (2003). The biosynthesis of L-arabinose in plants: molecular cloning and characterization of a Golgi-localized UDP-D-xylose 4-epimerase encoded by the *MUR4* gene of *Arabidopsis*. *Plant Cell* **15**, 523–531.

Campbell, G. R., Reuhs, B. L. & Walker, G. C. (2002). Chronic intracellular infection of alfalfa nodules by *Sinorhizobium meliloti* requires correct lipopolysaccharide core. *Proc Natl Acad Sci U S A* **99**, 3938–3943.

Carlson, R. W., Reuhs, B. L., Forsberg, L. S. & Kannenberg, E. L. (1999). Rhizobial cell surface carbohydrates: their structures,

biosynthesis and functions. In *Genetics of Bacterial Polysaccharides*, pp. 53–90. Edited by J. B. Goldberg. Boca Raton, FL: CRC Press.

De Leizaola, M. & Dedonder, R. (1955). Etude de quelques polyoisides produits par des souches de *Rhizobium*. *C R Hebd Seances Acad Sci* **240**, 1825–1827.

Egelund, J., Petersen, B. L., Motawia, M. S., Damager, I., Faik, A., Olsen, C. E., Ishii, T., Clausen, H., Ulvskov, P. & Geshi, N. (2006). *Arabidopsis thaliana RGXT1* and *RGXT2* encode Golgi-localized (1,3)-α-D-xylosyltransferases involved in the synthesis of pectic rhamnogalacturonan-II. *Plant Cell* **18**, 2593–2607.

Forsberg, L. S. & Carlson, R. W. (2008). Structural characterization of the primary O-antigenic polysaccharide of the *Rhizobium leguminosarum* 3841 lipopolysaccharide and identification of a new 3-acetimidoyl-amino-3-deoxyhexuronic acid glycosyl component: a unique *O*-methylated glycan of uniform size, containing 6-deoxy-3-*O*-methyl-D-talose, *N*-acetylquinovosamine, and rhizoaminuronic acid (3-acetimidoyl-amino-3-deoxy-D-gluco-hexuronic acid). *J Biol Chem* **283**, 16037–16050.

Gage, D. J. (2004). Infection and invasion of roots by symbiotic, nitrogen-fixing rhizobia during nodulation of temperate legumes. *Microbiol Mol Biol Rev* **68**, 280–300.

Galibert, F., Finan, T. M., Long, S. R., Puhler, A., Abola, P., Ampe, F., Barloy-Hubler, F., Barnett, M. J., Becker, A. & other authors (2001). The composite genome of the legume symbiont *Sinorhizobium meliloti*. *Science* **293**, 668–672.

Gatzeva-Topalova, P. Z., May, A. P. & Sousa, M. C. (2005). Structure and mechanism of ArnA: conformational change implies ordered dehydrogenase mechanism in key enzyme for polymyxin resistance. *Structure* **13**, 929–942.

Götting, C., Kuhn, J., Zahn, R., Brinkmann, T. & Kleesiek, K. (2000). Molecular cloning and expression of human UDP-D-xylose : proteoglycan core protein β-D-xylosyltransferase and its first isoform XT-II. *J Mol Biol* **304**, 517–528.

Gu, X., Glushka, J., Yin, Y., Xu, Y., Denny, T., Smith, J. A., Jiang, Y. & Bar-Peled, M. (2010). Identification of a bifunctional UDP-4-keto-pentose/UDP-xylose synthase in the plant pathogenic bacterium, *Ralstonia solanacearum* str. GMI1000: a distinct member of the 4,6-dehydratase and decarboxylase family. *J Biol Chem* **285**, 9030–9040.

Harper, A. D. & Bar-Peled, M. (2002). Biosynthesis of UDP-xylose. Cloning and characterization of a novel *Arabidopsis* gene family, *UXS*, encoding soluble and putative membrane-bound UDP-glucuronic acid decarboxylase isoforms. *Plant Physiol* **130**, 2188–2198.

Hirsch, A. M. (1999). Role of lectins (and rhizobial exopolysaccharides) in legume nodulation. *Curr Opin Plant Biol* **2**, 320–326.

Humphrey, B. A. & Vincent, J. M. (1959). Extracellular polysaccharides of *Rhizobium*. *J Gen Microbiol* **21**, 477–484.

Hwang, H. Y. & Horvitz, H. R. (2002). The SQV-1 UDP-glucuronic acid decarboxylase and the SQV-7 nucleotide-sugar transporter may act in the Golgi apparatus to affect *Caenorhabditis elegans* vulval morphogenesis and embryonic development. *Proc Natl Acad Sci U S A* **99**, 14218–14223.

Jones, K. M., Kobayashi, H., Davies, B. W., Taga, M. E. & Walker, G. C. (2007). How rhizobial symbionts invade plants: the *Sinorhizobium–Medicago* model. *Nat Rev Microbiol* **5**, 619–633.

Kannenberg, E. L. & Brewin, N. J. (1989). Expression of a cell surface antigen from *Rhizobium leguminosarum* 3841 is regulated by oxygen and pH. *J Bacteriol* **171**, 4543–4548.

Kannenberg, E. L. & Carlson, R. W. (2001). Lipid A and O-chain modifications cause *Rhizobium* lipopolysaccharides to become hydrophobic during bacteroid development. *Mol Microbiol* **39**, 379–391.

Kannenberg, E. L., Perotto, S., Bianciotto, V., Rathbun, E. A. & Brewin, N. J. (1994). Lipopolysaccharide epitope expression of *Rhizobium* bacteroids as revealed by in situ immunolabelling of pea root nodule sections. *J Bacteriol* **176**, 2021–2032.

Karr, D. B., Liang, R. T., Reuhs, B. L. & Emerich, D. W. (2000). Altered exopolysaccharides of *Bradyrhizobium japonicum* mutants correlate with impaired soybean lectin binding, but not with effective nodule formation. *Planta* **211**, 218–226.

Karunakaran, R., Ramachandran, V. K., Seaman, J. C., East, A. K., Mouhsine, B., Mauchline, T. H., Prell, J., Skeffington, A. & Poole, P. S. (2009). Transcriptomic analysis of *Rhizobium leguminosarum* biovar viciae in symbiosis with host plants *Pisum sativum* and *Vicia cracca*. *J Bacteriol* **191**, 4002–4014.

Keating, D. H., Willits, M. G. & Long, S. R. (2002). A *Sinorhizobium meliloti* lipopolysaccharide mutant altered in cell surface sulfation. *J Bacteriol* **184**, 6681–6689.

Klutts, J. S. & Doering, T. L. (2008). Cryptococcal xylosyltransferase 1 (Cxt1p) from *Cryptococcus neoformans* plays a direct role in the synthesis of capsule polysaccharides. *J Biol Chem* **283**, 14327–14334.

Konishi, T., Takeda, T., Miyazaki, Y., Ohnishi-Kameyama, M., Hayashi, T., O'Neill, M. A. & Ishii, T. (2007). A plant mutase that interconverts UDP-arabinofuranose and UDP-arabinopyranose. *Glycobiology* **17**, 345–354.

Kuhn, J., Götting, C., Schnolzer, M., Kempf, T., Brinkmann, T. & Kleesiek, K. (2001). First isolation of human UDP-D-xylose: proteoglycan core protein β-D-xylosyltransferase secreted from cultured JAR choriocarcinoma cells. *J Biol Chem* **276**, 4940–4947.

Laus, M. C., Logman, T. J., Van Brussel, A. A., Carlson, R. W., Azadi, P., Gao, M. Y. & Kijne, J. W. (2004). Involvement of exo5 in production of surface polysaccharides in *Rhizobium leguminosarum* and its role in nodulation of *Vicia sativa* subsp. *nigra*. *J Bacteriol* **186**, 6617–6625.

Pattathil, S., Harper, A. D. & Bar-Peled, M. (2005). Biosynthesis of UDP-xylose: characterization of membrane-bound AtUxs2. *Planta* **221**, 538–548.

Peña, M. J., Zhong, R., Zhou, G. K., Richardson, E. A., O'Neill, M. A., Darvill, A. G., York, W. S. & Ye, Z. H. (2007). *Arabidopsis irregular xylem8* and *irregular xylem9*: implications for the complexity of glucuronoxylan biosynthesis. *Plant Cell* **19**, 549–563.

Porchia, A. C., Sorensen, S. O. & Scheller, H. V. (2002). Arabinoxylan biosynthesis in wheat. Characterization of arabinosyltransferase activity in Golgi membranes. *Plant Physiol* **130**, 432–441.

Puvanesarajah, V., Schell, F. M., Gerhold, D. & Stacey, G. (1987). Cell surface polysaccharides from *Bradyrhizobium japonicum* and a nonnodulating mutant. *J Bacteriol* **169**, 137–141.

Ricke, S. C., Martin, S. A. & Nisbet, D. J. (1996). Ecology, metabolism, and genetics of ruminal selenomonads. *Crit Rev Microbiol* **22**, 27–56.

Sánchez-Andújar, B., Coronado, C., Philip-Hollingsworth, S., Dazzo, F. B. & Palomares, A. J. (1997). Structure and role in symbiosis of the *exoB* gene of *Rhizobium leguminosarum* bv trifolii. *Mol Gen Genet* **255**, 131–140.

Syn, C. K. & Swarup, S. (2000). A scalable protocol for the isolation of large-sized genomic DNA within an hour from several bacteria. *Anal Biochem* **278**, 86–90.

Thoden, J. B., Frey, P. A. & Holden, H. M. (1996). Molecular structure of the NADH/UDP-glucose abortive complex of UDP-galactose 4-epimerase from *Escherichia coli*: implications for the catalytic mechanism. *Biochemistry* **35**, 5137–5144.

van Rhijn, P. & Vanderleyden, J. (1995). The *Rhizobium*–plant symbiosis. *Microbiol Rev* **59**, 124–142.

Zhang, Q., Shirley, N., Lahnstein, J. & Fincher, G. B. (2005). Characterization and expression patterns of UDP-D-glucuronate decarboxylase genes in barley. *Plant Physiol* **138**, 131–141.

Edited by: A. S. Ball